International Journal of Smart Grid and Clean Energy

The employment of artificial neural network to predict the performance of an air to water heat pump

Stephen Tangwe*, Kusakana Kanzumba

Central University of Technology, P/SAK X20539, Bloemfontein, 9301, South Africa

Abstract

Air to water heat pump (AWHP) is an efficient and renewable technology for sanitary water heating. The study focused on the building and development of an artificial neural network (ANN) to predict the electrical energy consumed (E) and COP of a 1.2 kW split type AWHP with the volume of hot water drawn, ambient temperature, relative humidity, difference in refrigerant temperatures at the outlet and inlet of the compressor and at the inlet and outlet of the condenser as the input parameters. An ANN of 5-10-2 configuration with Levenberg-Marquardt as the variant of the back propagation algorithm was used to train the input and output dataset. The trained network shows that both the modelled outputs and the targets of the AWHP for the summer season mimic each other with a deviation of ±0.019. The correlation coefficients (R) for the training, validation and testing sample dataset with the trained network was 0.967, 0.962 and 0.945, respectively. The trained ANN was used to evaluate the network with an additional test dataset of the inputs and outputs that were not considered during the training of the ANN. The modelled outputs and targets for the evaluation network gave an excellent prediction with a correlation coefficient and mean square error of 0.996 and 0.003, respectively. We can conclude that the trained ANN is simple to configure and less time consuming in building and training the network, but, was capable of predicting both the E and COP of the AWHP with reasonably high accuracy with a 95% confidence level.

Keywords: Air to water heat pump, artificial neural network, correlation coefficient, coefficient of performance, levenberg-marguardt variant

Nomenclature

COP	Coefficient of performance
AWHP	Air to water heat pump
Ta	ambient temperature in °C
V	Volume of hot water drawn off in L
RH	Relative humidity in %
p	Average electrical power consumed in kW
t	Time taken in h
E	Electrical energy consumed in kWh
m	Mass of water heated by ASHP unit in kg
c	specific heat capacity of water in kJ/kg°C
Tconi	Refrigerant temperature at the inlet of condenser in °C
Tcono	Refrigerant temperature at the outlet of condenser in °C
Tcomi	Refrigerant temperature at the inlet of compressor in °C
Tcomo	Refrigerant temperature at the outlet of compressor in °C
To	Water temperature at the outlet of ASHP unit in °C
Ti	Water temperature at the inlet of ASHP unit in °C
Q	Output thermal energy gained by stored water in kWh
ANN	Artificial neural network

* Manuscript received June 6, 2021; revised November 17, 2021.
Corresponding author. *E-mail address*: lstephen@cut.ac.za.
doi: 10.12720/sgce.11.1.29-40

LM	Levenberg-Marguardt variant
MLFFN	Multi-layer feed forward network
MSE	Mean square error
R	correlation coefficient
ASHP	Air source heat pump unit

1. Introduction

A number of physics based thermofluid models and multiple linear regression models have been used to predict the performance of residential air to water heat pumps (AWHPs). These models are complex and time consuming in implementing. Therefore, artificial neural networks (ANNs) can be used to predict the performance of AWHPs with very high accuracy and are simple to develop as well as training of the networks. Bechtler et al. [1] used a generalized radial basis function (GRBF) neural network for predicting the steady-state performance of a vapour-compression liquid heat pump. The COP of a heat pump using R22, LPG (liquid petroleum gas) and R290 was predicted with reference to chilled water outlet temperature from the evaporator, cooling water inlet temperature of the condenser and evaporator capacity. The predictions of COP values, when R22 or LPG was used as a refrigerant are within 2% deviation compared to experimental values. However, the COP predictions of the heat pump system with R290 as refrigerant, show a deviation of more than ±10%. Researchers have predicted the performance of a heat pump system with different mass ratios of refrigerant mixture R12/R22 using ANN [2]. They developed a multi-layer feed forward network (MLFFN) with three neurons in the input layer representing the mixture ratio, the refrigerant temperature entering the evaporator and condenser pressure, and two neurons in the output layer representing COP and rational efficiency. Three variants such as Levenberg–Marquardt (LM), Conjugate Gradient Pola–Ribiere (CGP), and Scaled Conjugate Gradient (SCG) with log-sigmoid transfer function was used in their study. The network predictions of COP and rational efficiency are closer to experimental results with a determination coefficient of 0.9999. They also reported that the LM variant provided better results compared to CGP and SCG. Arcaklioglu [2] predicted the performance parameters of the system (COP and total irreversibility) using environment friendly alternative refrigerants. He developed a MLFFN with seven neurons in the input layer representing the mixture ratios of R32, R125, R134A, R143A, R152A, R290 and R600A and two neurons in the output layer representing the COP and total irreversibility. Three learning algorithms which were SCG, CGP and LM with logistic sigmoid transfer function were used in his work. The number of neurons was varied between 23 and 26. His results confirmed that the LM algorithm with 24 neurons in the hidden layer yields a maximum correlation coefficient of 0.9999 with a maximum error of less than 3% and root mean square error of 0.002. ANN technique was successfully applied in predicting the performance of a horizontal and vertical ground source heat pump water heaters [3; 4]. In reference to the study, the COP was predicted using three parameters such as air temperature entering the condenser unit, air temperature leaving the condenser unit and ground temperatures (at 1 and 2 m depth) as the input layer. The back propagation algorithm (BPA) using three different variants, namely LM, CGP and SCG with tangent sigmoid transfer functions was used in the network. It was reported that the LM learning algorithm with 3-7-1 configuration predicts the COP closer to the experimental results with a root mean square error of 1%, while the determination coefficient and covariance was 99.99% and 28.62% for the horizontal ground source heat pump water heater. Mohanraj et al. [5] developed an ANN model for energy performance prediction of a direct expansion solar assisted heat pump water heater. The performance parameters such as energy performance ratio, heating capacity, compressor discharge temperature and power consumption were predicted with reference to the solar intensity and ambient temperature. The ANN utilized the LM variant with a 2-10-4 configuration. The network predictions of the energy performance ratio, heating capacity, compressor discharge temperature and power consumption were closer to experimental measurements with root mean square errors of 0.0075, 17.28 W, 0.2258 ◦C and 5.6 W, respectively while the determination coefficient was above 0.9988 for all the predictions. Similarly, ANN was successfully applied in predicting the exergy destruction and exergy efficiency of a direct expansion solar assisted heat pump water heater [6]. The authors developed two ANNs for predicting the exergy destruction and exergy efficiency of each component of the system with reference to the solar intensity and ambient temperature. The two ANNs employed the LM variant and were optimized with 2-12-5 configuration. The ANN predictions were reported to be closer with experimental results with the determination coefficients of 0.9938, 0.9898, 0.9930, 0.9779 and 0.9933 and covariance of 1.53, 1.043, 0.0292, 0.9887 and 0.4361 for exergy of destruction in the compressor, condenser, expansion valve, solar collector and the overall system, respectively. In addition, the exergy efficiencies are closer to the experimental results with the determination coefficients of 0.9891, 0.9957, 0.999, 0.9517 and 0.9472 and covariance of 0.372, 0.7996, 0.0029, 1.2418 and 1.5624 for the compressor, condenser, expansion valve, solar collector and the overall system, respectively. Aktas et al. [7] used ANN to predict the performance of bay leaf drying using a heat pump fruit dryer. The ANN prediction and measured outputs of moisture content and total energy consumed by the heat pump fruit dryer with the input parameters (drying air temperature, drying air relative humidity and drying air velocity) give sufficient good accuracies with an absolute mean percentage error of less than 0.5. The determination coefficient were 0.996 and 0.997 while the root mean square error were 0.0002053 and 0.0005013, for the moisture content and the total energy consumed, respectively. The ANN was developed using a fermi transfer function with a 3-17-4-2 configuration and LM variant as the back propagation algorithm. Research has been conducted with ANN to modelled both the energy quantities and state properties with ambient temperature and cold water temperature as input parameters on a 280 L air source heat pump water heater [8]. The results depicted that the model outputs and the measured targets were of very good accuracies while using the 2-10-6 configuration with LM as the variant. The learning rate and the momentum factor were 0.3 and 0.9, respectively, while the sampling iteration was set to 1000. The trained air source heat pump water heater with inputs (air temperature at evaporator inlet and water temperature at condenser inlet) and outputs (thermal energy gained, COP, energy consumed by air source heat pump water heater, high pressure at discharge line of the compressor, low pressure at the suction line of the compressor and water temperature at the condenser outlet) gives high accuracies and the modelled outputs was closer to the targets. The correlation coefficients for each of the modelled outputs and targets was over 0.998, for the training, validation, testing and all data pattern scenarios. Schachtery and Mancarella [9] used the Feedforward artificial neural network (ANN) algorithms to forecast short term demand responses for both GSHP and HVAC systems in multiple sites in the United Kingdom. They confirmed that the ANN models give better predictions when tested against multiple linear regression models with reference to the values of the mean absolute percentage error and the correlation coefficient. Deb et al. [10] compared the performance of HVAC systems of 56 office buildings in Singapore with MLR model and an ANN whose predictors were energy consumption, operational hours, gross floor area and the chiller plant efficiency while the energy saving was the output. They concluded from their study that the ANN outperformed the MLR model in making prediction of the energy savings in the office buildings to be retrofitted. Li et al. [11] employed a clustering-based method for “cross-scale” load prediction on building levels with HVAC systems. They affirmed that the proposed model showed an excellent effectiveness and with better accuracy based on the validation with real-world data. Lin et al. [12] compared the MLR and the naïve Bayes classifier artificial neural network in the prediction of the HVAC energy consumption using hourly data and confirmed the latter gave a better accuracy in terms of the normalized mean bias error and the coefficient of variation of the root mean squared error.

2. Uncertainty Analysis of the Measurements

The temperature sensor used was a 12 bits S-TMB temperature sensor, with measurement range from -40 to 100 ºC and the accuracy was ±0.2 ºC. The ambient temperature and relative humidity sensor used was a 12 bits S-THB temperature and relative humidity sensor with a temperature range from 0 – 50 ºC and the accuracy was ±0.21 ºC, while the accuracy of the relative humidity was ±0.25% over the ranged 0 – 99%. The flow meter used was a T-Minol 130 flow meter and the measurement range from 1.0 to 100 L/min, with an accuracy between 97 and 99%. The power and energy meter used was a TVER-E50B2 power meter and was a class 2 power meter with an uncertainty error of 0.5%. The uncertainty in the data logger was negligible. The calculated uncertainty error of the COP and the electrical and thermal energies were ±0.203, ±0.091 and ±0.03 kWh, respectively.

3. Theory and Calculations

The input electrical energy consumed by the AWHP during the heating cycle is the product of the average electrical power consumed and the time taken. This is given in Equation 1.

$$E=pt \tag{1}$$

Where, E is the electrical energy consumed, p is the electrical power consumed and t is the time taken.

The output thermal energy gained by the stored hot water is the product of the mass of water heated by the ASHP unit, the specific heat capacity of water and the difference in water temperature between the outlet and inlet of the ASHP unit during the vapour compression refrigeration cycle as given by Equation 2.

$$Q=mc(To-Ti) \tag{2}$$

Where, Q is the thermal energy gained, m is the mass of water heated, c is the specific heat capacity of water, to is the water temperature at the outlet of the ASHP unit and Ti is the water temperature at the outlet of the ASHP unit.

The COP of the ASHP water heater is the ratio of the output thermal energy gained by the stored water and the input electrical energy consumed by the ASHP unit and is given by Equation 3.

$$COP=\frac{Q}{E} \tag{3}$$

Where, COP is the coefficient of performance, E is the electrical energy consumed and Q is the thermal energy gained.

The transfer functions used in the ANN is the log-sigmoid activation function and is given in Equation 4.

$$f(z)=\frac{1}{(1-e^{-z})} \tag{4}$$

Where, $z=f((\sum w_i\, x_i)$, i is the index on inputs to neuron, x_i is the input to neuron, w_i is the weighted factor attached to input, z is the weighted input.

The mean square error (MSE) is the square of the root mean square error (RMS) between the targets $(y_j)$and model output $(\hat{y}_j)$. The RMS is given in Equation 5.

$$RMS=\sqrt{\frac{1}{n}\sum_{j=1}^{n}\left(y_j-\hat{y}_j\right)^2} \tag{5}$$

Where; $j=1,\dots\dots,n$

The correlation coefficient (R) is the square root of the determination coefficient (R^2) between the actual outputs (y_j) and model output $(\hat{y}_j)$ and is given in Equation 6.

$$R^2=1-\frac{\sum_1^n\left(y_j-\hat{y}_j\right)^2}{\sum_1^n\left(y_j-\bar{y}\right)^2} \tag{6}$$

Where; $\bar{y}$ =mean of the actual output or target data

The uncertainties derived from the calculations, as a result of the error measurements from the set of independent variables were based on the formulation proposed by Meyer [13] and is given by Equation 7.

$$w_r = \left[\left[w_1 \frac{\partial R}{\partial X_1}\right]^2 + \left[w_2 \frac{\partial R}{\partial X_2}\right]^2 + \ldots\ldots\ldots\ldots + \left[w_n \frac{\partial R}{\partial X_n}\right]^2\right] \tag{7}$$

Where: R = The given function; w_r = total uncertainty; $X_1, X_2, \ldots\ldots X_n$ = Independent variables and $w_1, w_2, \ldots\ldots w_n$ = Uncertainty in the independent variables.

Sample size is a statistical method for the decision of the accurate experimental repetition value, and is given by Equation 8.

$$n = \frac{Z^2 \sigma^2}{d^2} \tag{8}$$

Where Z = 1.96 and is obtained from the confidence level at 95%; σ = 3, and is standard deviation obtained due to the preliminary studies of the system and d = margin of error of 5% and is assumed based on the expectations.

4. Materials and Methods

4.1. Materials

The list of materials used in the experiment are shown in Table 1.

Table 1. List of materials, both the devices and sensors

Item	Material	Quantity
1	1.2 kW split type ASHP unit	1
2	150 L , 3 kW high pressure geyser	1
3	Hot water volume control valve	1
4	Ambient temperature and relative humidity sensor	1
5	Power meter	1
6	Temperature sensors	11
7	Flow meter	1
8	Hot water collecting drum	1
9	Data logger	1
10	Weather and waterproof enclosure	1

4.2. Methods

The methods of the study are divided into four; namely,

- The experimental setup of the AWHP and the installation of the sensors
- The conduction of the hot water drawn off (50, 100 and 150 L) during the time of use for the summer period (January to April 2020).
- Analyses of the inputs and output(s) dataset and training of the ANN.
- Evaluation of the ANN, with an additional test dataset, to ascertain the validity of the ANN model.

4.3. Experimental Setup

Fig. 1 shows the installed AWHP used in the study and was deployed in a research and development facility owned by AET Africa in the Eastern Cape Province of South Africa.

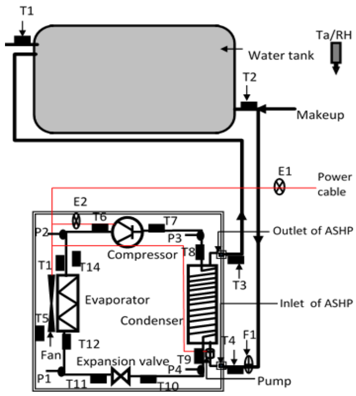

Fig. 1. Installed AWHP and the metering sensors

An ambient temperature and relative humidity sensor (Ta/RH) was installed in the vicinity of the AWHP and measured both the ambient temperature and relative humidity. A power meter (E1) was installed on the power cable supplying electricity to the ASHP unit and measured the input electrical energy of the AWHP. A flow meter (F1) was installed at the closed end of the inlet to the ASHP unit and measured the volume of hot water heated by the ASHP unit. Eleven temperature sensors were installed at different locations of the installed AWHP. Temperature sensor (T1) measured the temperature of the incoming cold water from the mains into the storage tank of the AWHP. Temperature sensor (T2) measured the temperature of the hot water drawn off into a calibrated 200 L drum. Temperature sensors (T4 and T3) measured the water temperatures at the inlet and outlet of the ASHP unit. Temperature sensors (T6 and T7) measured the refrigerant temperatures at the suction and the discharge ends of the ASHP's compressor. Temperature sensors (T8 and T9) measured the refrigerant temperatures at the inlet and the outlet of the ASHP's condenser. All the sensors and the transducers were accommodated into 15 channel data logger and were products of the Hobo corporation. These sensors and transducers were configured by the hoboware pro software to log in 5 minute interval throughout the experiment [14].

5. Results and Discussion

5.1. Summer Electrical and Thermo-Physical Properties of the AWHP

Table 2, shows samples of observations of the measured inputs and determined targets for the summer months.

Table 2. Observations of inputs and targets recorded

Observations	V/L	Ta/ºC	RH/%	ΔTcom/ºC	ΔTcon/ºC	E/kWh	COP
1	50	20.45	85.61	49.16	35.27	0.91	2.35
2	100	17.57	91.38	48.46	35.53	1.41	2.58
3	150	29.18	41.50	46.90	41.52	1.43	2.95
4	150	18.35	85.18	47.89	34.90	1.47	2.78
5	100	17.57	91.38	48.46	35.53	1.41	2.58
6	50	20.45	85.61	49.16	35.27	0.91	2.35
7	100	23.29	75.05	48.44	37.95	1.34	2.49
8	150	19.98	76.12	48.28	37.69	1.73	3.01
9	50	18.81	86.05	38.94	27.34	1.03	2.76
10	150	24.79	39.40	46.09	40.14	1.89	3.01
11	150	16.43	72.25	46.68	35.08	2.15	3.35

V =Volume of hot water drawn off, Ta =Ambient temperature, RH=Relative humidity, ΔTcom =Difference between refrigerant temperature at the outlet and inlet of compressor, ΔTcon =Difference between refrigerant temperature at the inlet and outlet of condenser, E=Electrical energy consumed, COP=Coefficient of performance

It can be depicted that the ambient temperatures range from 16 to 30 ^{o}C while the relative humidity was between 41 and 92% during the heating cycles of the AWHP. The average lowest electrical energy consumed and the COP was 0.91 kWh and 2.35 and occurred after a 50 L hot water drawn off. In addition, the maximum electrical energy consumed and the COP was 2.15 kWh and 3.35 and occurred after a 150 L hot water drawn off. The change in refrigerant temperatures between the outlet and the inlet of the compressor was between 38 and 49 ^{o}C. The change in refrigerant temperatures between the inlet and outlet of the condenser was between 35 and 40 ^{o}C. Hence, the refrigerant temperature difference was higher in the compressor than in the condenser. Although, the COP depends on the ambient temperature, it is also influenced by the initial water temperature in the water tank.

5.2. Training, validation and testing dataset performance obtained from the trained ANN

The analysed dataset for the inputs and output(s) are partition in the developed and built ANN model into 60, 20 and 20% of training, validation and testing samples. Table 3 shows the mean square error (MSE) and the correlation coefficient (R) for the training, validation, and testing samples obtained from the trained neural network. The very small values of MSE closer to 0 and the excellent values of R closer to 1, justified that the predicting model outputs (COP and E) are of high accuracies for the training, validation and testing sample dataset.

Table 3. MSE and R of the trained ANN

	Samples	**MSE**	**R**
Training	18	0.0393	0.967
Validation	6	0.0389	0.962
Testing	6	0.078	0.954

MSE=Mean square error, R=Correlation coefficient

Fig. 2, shows the regression plots of the modelled outputs and the targets for the training, validation, testing and all data pattern obtained with the trained ANN model. The results in all four regression plots demonstrated very strong correlation coefficients between the modelled line and best fit and were over 0.980. Hence, the trained ANN is accepted in predicting the E and the COP of the experimental split type AWHP.

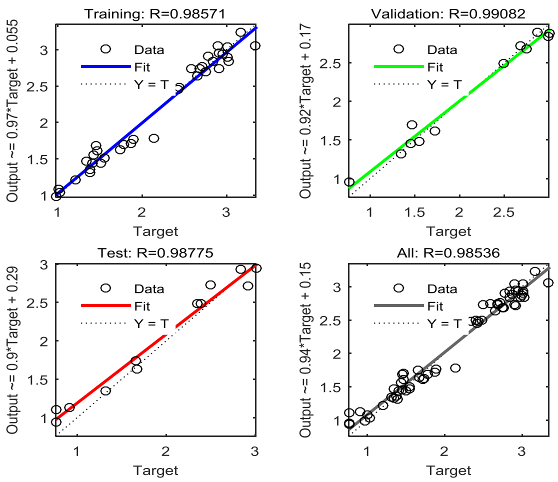

Fig. 2. Regression plots for the model output and target for training, validation and test samples

The performance of the trained ANN model is shown in Fig. 3. The best validation performance was achieved when the MSE was 0.0126 at epoch of 3 after 9 iterations. It is worthy to note that the sampling iteration for the trained ANN was set at 1000, as a default. It is observed that at the best performance validation, the minimization of the error between the model and the target stop improving. A further training of the network will result in decreasing the accuracy of the trained ANN. The testing samples have no influenced on the training network, as only the validation samples are used to compare with the training sample, in the process of minimization of the modelled outputs and the targets.

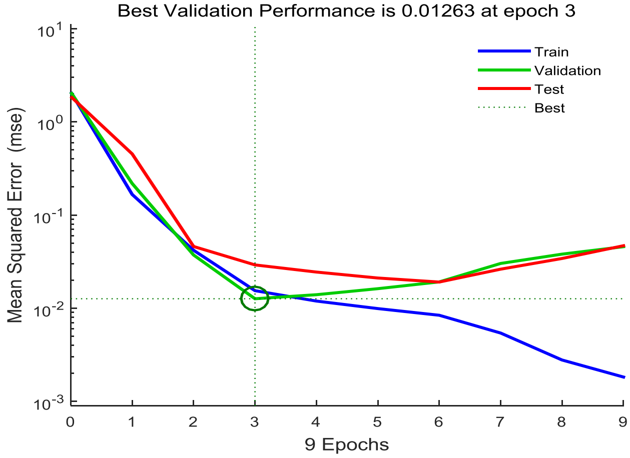

Fig. 3. The trained ANN used in prediction of best performance

5.3. Evaluation of the network

Additional test samples of the dataset not used in the training of the ANN were used to evaluate the trained network. Fig. 4, shows the regression plot for the modelled line and the test targets. It can be depicted that the validation gave a very good prediction, whereby the R and the MSE of the targets and the modelled outputs with the test dataset was 0.996 and 0.003, respectively. Also, the best fit and the trained modelled line were in very good agreement and the R was 0.9995.

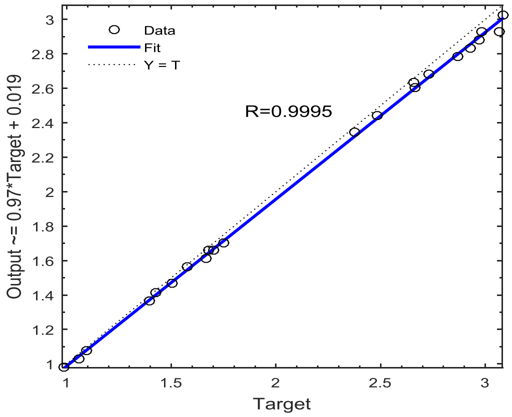

Fig. 4. The trained ANN and evaluation dataset

Figs. 5 and 6, show the correlation of each of the outputs (E and COP) for the evaluated test samples and their corresponding modelled curve from the trained ANN. It was determined that both the outputs for the evaluation samples and the corresponding modelled curves derived from the trained ANN had very good R of 0.9999. In Fig 6, the sample dataset of the test COPs ranged from 2.25 – 3.01 and the overall deviation between the trained network and the evaluated test dataset of COP values was less than 1%. In addition, the sample dataset of the test electrical energy consumed was between 0.95 and 1.74. It was determined that the deviation of the trained ANN model and the sample test dataset of the electrical energy consumed was 0.8%.

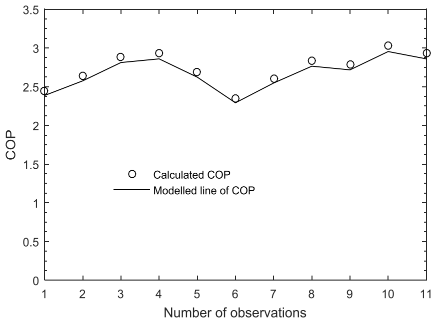

Fig. 5. Test dataset and trained ANN for COP

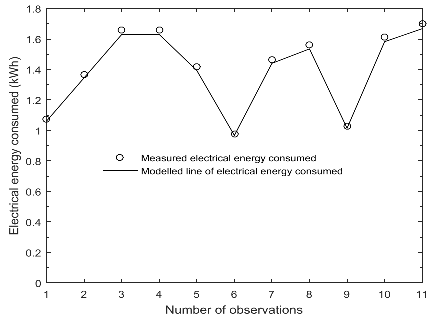

Fig. 6. Test dataset and trained ANN for electrical energy

5.4. Development of simulation application using the trained ANN

The trained ANN of the COP and E as the outputs and the set of predictors (V, Ta. RH, ΔTcom and ΔTcon) was embedded as a function fitting neural network in the Simulink environment of MATLAB and is shown in Fig. 7. The inputs are represented by the source ports and contained all the predictors (shown as constant in Simulink) while the outputs is represented by a sink port which displayed the result of the COP and E. The input of a specific predictor is varied over a unit steps and the predicted outputs were displayed on the scope after combining with the embedded trained ANN function. The volume of hot water drawn off was varied from 50 to 150 L, with a step of 50 L increment and the derived COP and E are displayed on the scope, while the other predictors were held constant (Ta=20 ºC, RH=70%, ΔTcom = 40 ºC and ΔTcon=35 ºC). The ambient temperature was changed from 10 to 37 ºC, with a unit increment and the derived COP and E are displayed on the scope, while the other predictors remained constant (V =100 L, RH=70%, ΔTcom = 40oc and ΔTcon=35 ºC). The relative humidity varied from 50 to 100%, with a 1% increment and the derived COP and E is displayed on the scope, while the other predictors remain unchanged (V=100 L, Ta =20 ºC, ΔTcom = 40 ºC and ΔTcon =35 ºC). The difference in the outlet and inlet refrigerant temperature at the compressor was varied from 10 to 55 ºC at a 1 ºC interval and the determined COP and E displayed on the scope while the other predictors were unchanged (V=100 L, Ta =20 ºC, RH=70% and ΔTcon =35 ºC). The difference in the inlet and outlet refrigerant temperature at the condenser was varied from 5 to 50 ºC at a unit increment and the determined COP and E displayed on the scope while the other predictors were invariant (V=100 L, Ta =20 ºC, RH=70% and ΔTcom =40 ºC).

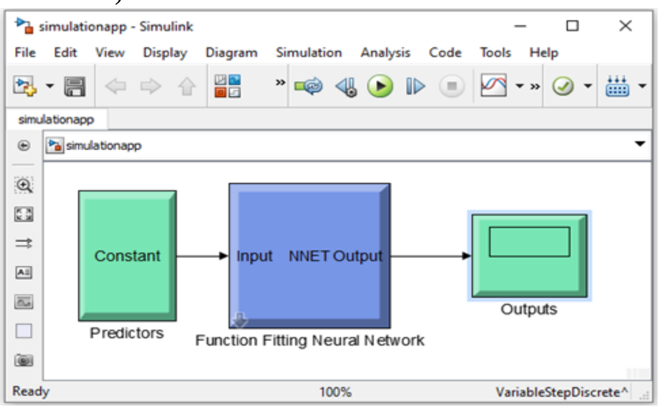

Fig. 7. Simulation application for the trained COP and E

5.5. 2D Multiple plots simulation used to demonstrate the variation of each predictor to train outputs

The generated inputs and determined outputs dataset from the simulation are represented in the 2D multiple surface model plots shown in Figs. 8 and 9. The 2D multiple surface model plots show the predicted output with the variation of a specific predictor while the others are held constant and is represented by the green lines. The broken red lines show the 95% confidence bound of the specific input's variability with the predicted output. Fig. 8 shows the 2D multiple surface model plots for the predictors and the predicted COP. Fig. 8, shows that the was a direct proportionality between V and the predicted COP and also between ΔTcon and the predicted COP, with correlation coefficients of 0.800 and 0.8104, respectively. Alternatively, there existed an inverse linear correlation between Ta and the predicted COP, RH and the predicted COP, as well as ΔTcom and the predicted COP, and the correlation coefficients were 0.9757, 0.8748 and 0.8104, respectively.

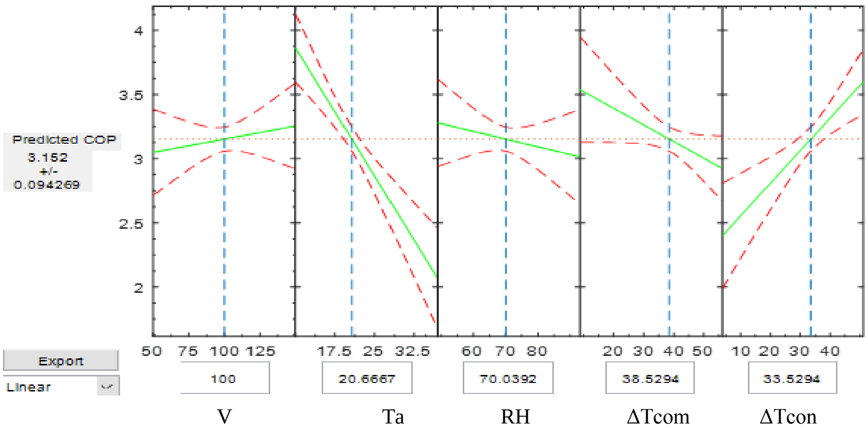

Fig. 8. 2D multiple surface model plots of predictors and predicted COP

Fig. 9 shows the 2D multiple surface model plots for the predictors and the predicted E. Fig. 9, revealed that the was a direct linear correlation between V and the predicted E, ΔTcom and the predicted E, and ΔTcon and the predicted E with correlation coefficients of 0.9921, 0.5537 and 0.9107 respectively. On the other hand, there were inverse linear correlation between Ta and the predicted E, and RH and the predicted E with correlation coefficients of 0.9944 and 0.9805, respectively.

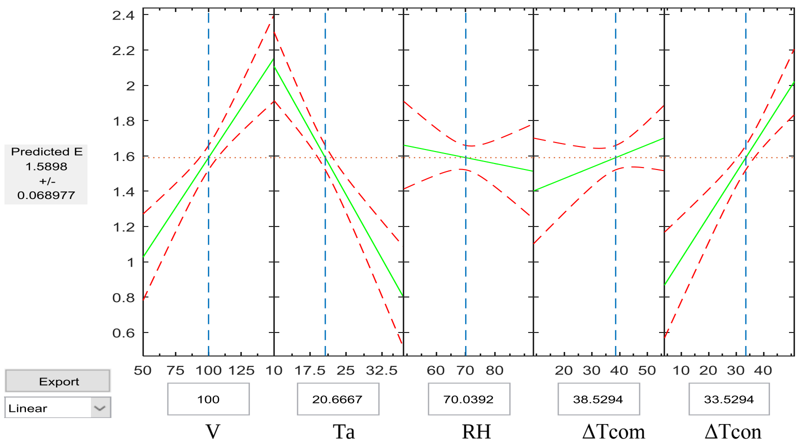

Fig. 9. 2D multiple surface model plots of predictors and predicted E

5.6. Ranking of predictors according to weight of importance to the outputs

The predictors were ranked according to their importance by weight of contribution to the output using the reliefF test. The reliefF test ranked the predictors according to the weight of contribution to the output using the regression method with the weights of the predictors ranging from -1 to 1. The negative weights are attributed to secondary input factors while the positive weights are associated with primary input factors.

The ranking of the predictors by weights of importance to the COP were Ta = 0.0970, ΔTcon = 0.0585, ΔTcom = -0.0026, RH = -0.0319 and V = -0.033 with a corresponding percentage of contribution to the predicted COP of 23.068, 21.580, 19.219, 18.087 and 18.045%, respectively. Hence, the predictor with the maximum percentage contribution was Ta while V had the minimum contribution by percentage. The ranking of the predictors by weights of importance to the E were Ta = 0.0728, ΔTcon = 0.0562, V = 0.0327, ΔTcom = 0.0024, and RH =-0.0447. And the percentage of contribution of Ta, ΔTcon, V, ΔTcom and RH to the predicted E was 21.8676, 21.2339, 20.3367, 19.1800 and 17.3818%, respectively. The predictor with the greatest contribution by percentage was Ta while the least was RH.

6. Conclusion

It can be concluded that a trained ANN with 5-10-2 configuration and the LM variant was used to predict the electrical energy consumed and the COP of the AWHP. The both E and COP predictions using the trained ANN gave an excellent R of over 95%. Furthermore, the trained ANN model and the actual measured datasets for both the COP and the electrical energy consumed demonstrated very high R of 0.967, 0.962 and 0.954, and excellent MSE of 0.0393,0.0389 and 0.078, for the training, validation and testing dataset. The 2D multiple surface model plots were used to demonstrate the variation of each predictor to the model outputs (E and COP) of the AWHP. In addition, the reliefF test were employed in ranking the predictors according to their weight of contributions to the desired outputs (E and COP) of the AWHP. The ANN was easy to train and configured and does not require any knowledge of the physics based thermofluid models, thermodynamics and fluid mechanics laws in the building and training of the network. The ANN models can be used for both performance assessment and optimization of the AWHP. All the predictors were ranked by weight of contribution into primary and secondary factors to the predicted COP and E.

Conflict of Interest

All authors declared no conflict of interest in the paper.

Author Contributions

Dr Stephen Tangwe was responsible of conceptualization, drafting and development of the manuscript. Prof K Kusakana provide technical input and conduct technical restructuring and proofreading of the manuscript.

Acknowledgements

We acknowledged the Centre for Sustainable SMART Cities, Central University of Technology, in Free State, South Africa for the financial supports.

References

[1] Bacthler H, Browne MW, Bansal PK, Kecman V. Neural networks—A new approach to model vapour compression heat pumps. *International Journal of Energy Research*, 2001;25:591–9.

[2] Arcaklioglu E, Erisen A, Yilmaz R. Artificial neural network analysis of heat pumps using refrigerant mixtures. *Energy Conversion Management*, 2004;45:1917–29.

[3] Esen H, Inalli M, Sengur A, Esen M. Performance prediction of a ground coupled heat pump system using artificial neural networks. *Expert Systems with Applications*, 2008;35:1940–8.

[4] Esen H, Inalli M. Modelling of a vertical ground coupled heat pump system by using artificial neural networks. *Expert Systems with Applications*, 2009;36:10229–1038.

[5] Mohanraj M, Jayaraj S, Muraleedharan C. Performance prediction of a direct expansion solar assisted heat pump using artificial neural networks. Applied Energy, 2009;86:1441–9.

[6] Mohanraj M, Jayaraj S, Muraleedharan C. Exergy assessment of direct expansion solar assisted heat pump working with R22 and R407C/LPG mixture. *International Journal of Green Energy*, 2010;7:65–83.

[7] Aktas N, Croci E, and Petmezas D. Is working capital management value-enhancing? Evidence from firm performance and investments. *Journal of Corporate Finance*, 2015; 30: 98-113

[8] Mathioulakis E, Panaras G, and Belessiotis V. Artificial neural networks for the performance prediction of heat pump hot water heaters. *International Journal of Sustainable Energy*, 2018; 37(2): 173-192.

[9] Schachter JYP, Mancarella. A short-term load forecasting model for demand response applications. en 11th International Conference on the European Energy Market (EEM14), 2014 May; 1-5.

[10] Deb C, Lee SE, Santamouris YM. Using artificial neural networks to assess HVAC related energy saving in retrofitted office buildings. *Sol. Energy*, Mar. 2018; 163: 32-44,.

[11] Li W, Gong G, Fan H, Peng P, Chun L, Fang YX. A clustering-based approach for “cross-scale” load prediction on building level in HVAC systems. *Appl. Energy*, 2021; 282: 116223.

[12] Lin CM, Lin SF, Liu HY, Tseng YKY. Applying the naïve Bayes classifier to HVAC energy prediction using hourly data. *Microsyst. Technol*., June 2019.

[13] Meyer SL. *Data Analysis for Scientists and Engineers*. Wiley, 1975.

[14] Onsetcomp. [Online]. Available: http://www.onsetcomp.com

Copyright © 2022 by the authors. This is an open access article distributed under the Creative Commons Attribution License (CC BY-NC-ND 4.0), which permits use, distribution and reproduction in any medium, provided that the article is properly cited, the use is non-commercial and no modifications or adaptations are made.